THE JOURNAL OF BIOLOGICAL CHEMISTRY VOL. 289, NO. 10, pp. 6839–6849, March 7, 2014

Functional Cross-talk between Ras and Rho Pathways

A Ras-SPECIFIC GTPase-ACTIVATING PROTEIN (p120RasGAP) COMPETITIVELY INHIBITS THE RhoGAP ACTIVITY OF DELETED IN LIVER CANCER (DLC) TUMOR SUPPRESSOR BY MASKING THE CATALYTIC ARGININE FINGER[*]

Received for publication, October 16, 2013, and in revised form, December 18, 2013 Published, JBC Papers in Press, January 17, 2014, DOI 10.1074/jbc.M113.527655

Mamta Jaiswal[‡1], Radovan Dvorsky[‡], Ehsan Amin[‡], Sarah L. Risse[‡], Eyad K. Fansa[‡], Si-Cai Zhang[‡], Mohamed S. Taha[‡], Aziz R. Gauhar[‡2], Saeideh Nakhaei-Rad[‡], Claus Kordes[§], Katja T. Koessmeier[‡], Ion C. Cirstea[‡¶], Monilola A. Olayioye[‖3], Dieter Häussinger[§], and Mohammad R. Ahmadian[‡4]

From the [‡]Institute of Biochemistry and Molecular Biology II and [§]Clinic for Gastroenterology, Hepatology and Infectiology, Medical Faculty, Heinrich Heine University, 40225 Düsseldorf, [¶]Leibniz Institute for Age Research, 07745 Jena, and [‖]Institute of Cell Biology and Immunology, University of Stuttgart, 70569 Stuttgart, Germany

Background: The regulatory mechanism of the DLC1 tumor suppressor protein is unclear.
Results: Structure-function analysis revealed determinants for the selectivity, activity, and inhibition of DLC1 RhoGAP function.
Conclusion: p120RasGAP competitively and selectively inhibits DLC1 by targeting its catalytic arginine finger.
Significance: This mechanistic study emphasizes the importance of the functional inter-relationships of GTPase-activating proteins mediating cross-talk between the Ras and Rho pathways.

The three deleted in liver cancer genes (DLC1–3) encode Rho-specific GTPase-activating proteins (RhoGAPs). Their expression is frequently silenced in a variety of cancers. The RhoGAP activity, which is required for full DLC-dependent tumor suppressor activity, can be inhibited by the Src homology 3 (SH3) domain of a Ras-specific GAP (p120RasGAP). Here, we comprehensively investigated the molecular mechanism underlying cross-talk between two distinct regulators of small GTP-binding proteins using structural and biochemical methods. We demonstrate that only the SH3 domain of p120 selectively inhibits the RhoGAP activity of all three DLC isoforms as compared with a large set of other representative SH3 or RhoGAP proteins. Structural and mutational analyses provide new insights into a putative interaction mode of the p120 SH3 domain with the DLC1 RhoGAP domain that is atypical and does not follow the classical P*XX*P-directed interaction. Hence, p120 associates with the DLC1 RhoGAP domain by targeting the catalytic arginine finger and thus by competitively and very potently inhibiting RhoGAP activity. The novel findings of this study shed light on the molecular mechanisms underlying the DLC inhibitory effects of p120 and suggest a functional cross-talk between Ras and Rho proteins at the level of regulatory proteins.

The Ras and Rho families of small GTP-binding proteins are key transducers of a variety of cellular processes ranging from reorganization of the cytoskeleton to transcriptional regulation and control of cell growth and survival (1). Loss of the control mechanisms and aberrant activation of Ras and Rho proteins are one of the most common molecular alterations found in cancer cells promoting tumor growth and metastasis (2–5). Ras signaling stimulates diverse pathways and signals toward Rho proteins, which are known to be required for cell transformation by oncogenic Ras (6–8). Emerging evidence suggests that the GTPase-activating proteins (GAPs),[5] in particular p120RasGAP (also known as RAS p21 protein activator 1 or RASA1; here called p120) and the Rho-specific p190ARhoGAP (also known as ARHGAP35; here called p190), p200RhoGAP (also known as ARHGAP32, p250GAP, GC-GAP, Rics, or Grit) and deleted in liver cancer 1 (DLC1; also known as ARHGAP7, p122RhoGAP, or STARD12), act as a linker between Ras and Rho signaling pathways (9–11). GAPs are multifaceted and multifunctional molecules (12, 13) and are the principal inactivators of Ras and Rho signaling. They utilize a catalytic "arginine finger" to stimulate the inefficient intrinsic GTP hydrolysis reaction of these small GTP-binding proteins by several orders of magnitude (14).

* This work was supported in part by the German Research Foundation (Deutsche Forschungsgemeinschaft (DFG)) through the Collaborative Research Center 974 (SFB 974) "Communication and Systems Relevance during Liver Injury and Regeneration," the International Research Training Group 1902 (IRGT1902), and Project Grant AH 92/5-1; the National Genome Research Network Plus program of the German Ministry of Science and Education (Bundesministerium für Bildung und Forschung Grant 01GS08100); and the International North Rhine-Westphalia Research School BioStruct granted by the Ministry of Innovation, Science and Research of the State North Rhine-Westphalia, the Heinrich Heine University of Düsseldorf, and the Entrepreneur Foundation at the Heinrich Heine University of Düsseldorf.

[1] Present address: Structural Biology Group, Max Planck Inst. for Molecular Physiology, Otto-Hahn-Strasse 11, 44227 Dortmund, Germany.
[2] Present address: Inst. of Physical Biology, Heinrich Heine University, 40255 Düsseldorf, Germany.
[3] Supported by the DFG Heisenberg program.
[4] To whom correspondence should be addressed: Inst. für Biochemie und Molekularbiologie II, Medizinische Fakultät der Heinrich-Heine-Universität, Universitätsstrasse 1, Gebäude 22.03, 40255 Düsseldorf, Germany. Tel.: 49-211-811-2384; Fax: 49-211-811-2726; E-mail: reza.ahmadian@uni-duesseldorf.de.

[5] The abbreviations used are: GAP, GTPase-activating protein; DLC, deleted in liver cancer; SH, Src homology; SAM, sterile α motif; START, steroidogenic acute regulatory related lipid transfer; aa, amino acids; tamra, tetramethylrhodamine; aSEC, analytical size exclusion chromatography; ITC, isothermal titration calorimetry.

Frequent loss of *DLC1* gene expression was first described in liver cancer (15) and later in breast, colon, gastric, prostate, cervical, esophageal, and other cancers (16–18). DLC1 RhoGAP function is required for the maintenance of cell morphology and the coordination of cell migration (11, 19–21). DLC1 and its isoforms DLC2 (also known as ARHGAP37 or STARD13) and DLC3 (also known as ARHGAP38 or STARD8) consist of an N-terminal sterile α motif (SAM) domain, a central phosphorylation region followed by the catalytic RhoGAP domain, and a C-terminal steroidogenic acute regulatory related lipid transfer (START) domain (see Fig. 1*A*) (22, 23). The SAM and GAP domains are linked by a serine-containing region, which contains a recognition motif for the phosphoserine/phosphothreonine-binding 14-3-3 adaptor proteins (22). DLC1 has been reported to interact with tensin, talin, focal adhesion kinase, and α-catenin (22, 24–29) and with lipids (30). However, the precise mechanism of DLC1 regulation remains unclear.

An emerging theme is that RhoGAPs, such as the OPHN1 and GRAF1 (31, 32) and p50RhoGAP (33–36), require activation through the relief of autoinhibitory elements. These elements are collectively membrane-binding modules, including BAR (Bin/Amphiphysin/Rvs), PH (pleckstrin homology), C1, and Sec14 domains (31–33, 36). The SAM domain of DLC1 has been suggested to act as an autoinhibitory domain of DLC1 RhoGAP activity *in vitro* and *in vivo*. SAM domain-deleted DLC1 displayed enhanced catalytic activity for RhoA (20). However, it is still unclear how such an autoregulatory mechanism of DLC1 may operate.

p120 contains multiple domains with different functions (see Fig. 1*B*) (37). Whereas the C terminus of p120 with the catalytic GAP activity is responsible for Ras inactivation (38–40), its N-terminal Src homology 2 and 3 (SH2 and SH3) domains have been suggested to possess an effector function (41–44). p120 functionally modulates Rho signaling by direct binding to two Rho-specific GAPs, p190 and DLC1 (9, 11, 45). The association of p120 with the tyrosine phosphorylated p190 via its SH2 domain promotes Rho inactivation (45–47). Thus, p120 positively regulates the RhoGAP function of p190. Another mechanism, which connects the Ras and Rho pathways and regulates the actin cytoskeleton, is dependent on the p120 SH3 domain and controls Rho activation (41). This mechanism was later revealed to involve DLC1 but not p190 (11). Here, the p120 SH3 domain (called $p120^{SH3}$) binds to the RhoGAP domain of DLC1 (called $DLC1^{GAP}$) and inhibits the DLC1-dependent Rho inactivation (11). Hereby, p120 acts as a negative regulator not only for Ras but also for the GAP activity of DLC1. However, the molecular mechanisms underlying these cross-talk phenomena have not yet been elucidated.

In this study, we have explored the regulatory mechanism of DLC1 at the molecular level, in particular its *trans*-inhibition by $p120^{SH3}$. We have characterized the selectivity of the interaction between the $DLC1^{GAP}$ and $p120^{SH3}$ using a large number of purified SH3 and RhoGAP proteins and identified structural and functional determinants for the DLC1-p120 interaction. This study provides deep insights into the underlying regulatory cross-talk between the Rho and Ras family of small GTP-binding proteins.

EXPERIMENTAL PROCEDURES

Constructs—Human Abr^{GAP} (aa 559–822), $DLC1^{fl}$ (aa 1–1091), $DLC1^{GAP}$ (aa 609–878), $DLC1^{SAM}$ (aa 1–96), $DLC1^{START}$ (aa 880–1079), $DLC2^{GAP}$ (aa 644–916), $DLC3^{GAP}$ (aa 620–890), $GRAF1^{GAP}$ (aa 383–583), $MgcRac^{GAP}$ (aa 343–620), $Nadrin^{GAP}$ (aa 245–499), $OPHN1^{GAP}$ (aa 375–583), $p50^{GAP}$ (aa 198–439), $p190^{GAP}$ (aa 1250–1513), N-terminal truncated $p120^{\Delta n128}$ (aa 129–1047); SH2-SH3-SH2-encoding $p120^{SH2\text{-}3\text{-}2}$ (aa 129–447), $p120^{SH3}$ (aa 275–350), Src^{SH3} (aa 77–140), and human RhoA (aa 1–181), Cdc42 (aa 1–178), and Rac1 (aa 1–184) were amplified by standard PCR and cloned in pGEX-4T1 and pGEX-4T1-NTEV, respectively. Constructs of SH3 domain of $Crk1^{SH3}$ (aa 131–191), $Grb2^{SH3\text{-}1}$ (aa 1–55), $Grb2^{SH3\text{-}2}$ (aa 159–217), $Nck1^{SH3\text{-}1}$ (aa 5–60), $Nck1^{SH3\text{-}2}$ (aa 109–163), and $Nck1^{SH3\text{-}3}$ (aa 173–262) were created as described previously (48).

Site-directed Mutagenesis—Point mutations N311R; L313A; W319G; and N311R,L313A,W319G in $p120^{SH3}$ and R677A in $DLC1^{GAP}$ were generated using the QuikChange™ site-directed mutagenesis kit (Stratagene) and confirmed by DNA sequencing.

Proteins—Escherichia coli BL21(DE3) pLysS, BL21(DE3) CodonPlus-RIL, and Rosetta(DE3) strains containing the respective plasmids (see constructs) were grown to an A_{600} of 0.7 (37 °C at 140 rpm) and induced with 0.1 mM isopropyl β-D-thiogalactopyranoside overnight at 25 °C as described before (49, 50). All proteins were isolated in a first step as glutathione *S*-transferase (GST) fusion proteins by affinity chromatography on a GSH-agarose column and in a second step by size exclusion chromatography (Superdex S75 or S200) after proteolytic cleavage of GST. GTP-binding proteins without nucleotide (nucleotide-free form) or with tetramethylrhodamine-conjugated GTP (tamraGTP) were prepared as described before (49, 50). Concentrations of proteins were determined by Bradford assay or absorbance at 280 nm using the extinction coefficient deduced from the protein sequence. Purified proteins were snap frozen in liquid nitrogen and stored at −80 °C.

Analytical Size Exclusion Chromatography (aSEC)—aSEC for the detection of complex formation was performed for $DLC1^{GAP}$ and $p120^{SH3}$ on a Superdex 75 column (10/300) using buffer containing 30 mM HEPES, pH 7.6, 5 mM $MgCl_2$, 150 mM NaCl, and 3 mM DTT. 10 μM $DLC1^{GAP}$ was incubated with 15 μM $p120^{SH3}$ for 5 min at 4 °C in the same buffer in a total volume of 150 μl. Before loading to an aSEC column, samples were spun at 13,000 rpm at 4 °C to remove any particulate impurities. The flow rate was maintained at 0.5 ml/min, and 500-μl fractions were collected. Peak fractions were visualized by 15% SDS-PAGE and subsequent Coomassie Blue staining.

Kinetics Measurements—All fluorescence measurements were performed at 25 °C in a buffer containing 30 mM Tris-HCl, pH 7.5, 10 mM K_2HPO_4/KH_2PO_4, pH 7.4, 10 mM $MgCl_2$, and 3 mM DTT. The tamraGTP hydrolysis of Rho proteins (0.2 μM) was measured in the absence and presence of different amounts of respective GAP proteins as described previously (49, 52). Fast kinetics (<1000 s) were performed with a Hi-Tech Scientific SF-61 stopped-flow instrument with a mercury xenon light source and TgK Scientific Kinetic Studio software (version

2.19). An excitation wavelength of 545 nm was used for tamra. Emission was detected through a cutoff filter of 570 nm. Slow kinetics (>1000 s) were measured on a PerkinElmer Life Sciences spectrofluorometer (LS50B) using an excitation wavelength of 545 nm and an emission wavelength of 583 nm. Data were evaluated by single exponential fitting with the GraFit program to obtain the observed rate constant (k_{obs}) for the respective reaction as described before (49, 52).

Isothermal Titration Calorimetry (ITC) Measurements—The interaction of $DLC1^{GAP}$ and $p120^{SH3}$ and analysis of $DLC1^{GAP}$ variant and different $p120^{SH3}$ variants were studied by ITC (MicroCal^{TM} VP-ITC microcalorimeter) as described (48). All measurements were carried out in 30 mM Tris-HCl, pH 7.5, 150 mM NaCl, 5 mM $MgCl_2$, and 1 mM tris(2-carboxyethyl)phosphine hydrochloride. The data were analyzed using Origin 7.0 software provided by the manufacturer.

Structural Analysis—To obtain insight into the residues responsible for the binding of the SH3 domain of p120 and RhoGAP domain of DLC1, docking of their corresponding structures (Protein Data Bank code 2J05 (53) and Protein Data Bank code 3KUQ, respectively), was performed with the program PatchDock (54). From the 20 best scored models, we selected the lowest energy model, which also has the Arg finger Arg-677 at the interface, and used it for further refinement with the program CHARMM (55). As the arginine finger is assumed to be crucial for the formation of the complex, we thoroughly explored its conformation in the course of refinement. Torsion angles of its side chain were additionally set up according to the Dynameomics rotamer library (56), and the energy of each complex was minimized by 2000 steps using the adapted basis Newton-Raphson method.

RESULTS

Low GAP Activities of the DLC Isoforms—Real time kinetic measurements of the RhoGAP activities of the DLC isoforms toward Cdc42, Rac1, and RhoA were performed using purified RhoGAP domains of the DLC proteins (Fig. 1) and fluorescent tamraGTP. This GTP analog is sensitive toward conformational changes induced by GTP hydrolysis (52). As shown in Fig. 2*A*, the very slow intrinsic tamraGTP hydrolysis of Cdc42 (*inset*) was markedly increased in the presence of the RhoGAP domain of DLC1 ($DLC1^{GAP}$). Similar experiments were performed under the same conditions with Rac1 and RhoA (Fig. 2*B*). Observed rate constants (k_{obs}) of respective $DLC1^{GAP}$ activities are presented in comparison with intrinsic hydrolysis rates as *bars* in Fig. 2*B*. $DLC1^{GAP}$ exhibited the highest activity for RhoA (1,650-fold) and Cdc42 (332-fold) and the lowest activity for Rac1 (75-fold). We next focused on the differences among the DLC isoforms and measured the activities of DLC2 and DLC3 for Cdc42 (Fig. 2*C*). Obtained data show that DLC2 and DLC3 exhibit 78- and 11-fold lower GAP activities, respectively, as compared with that of DLC1. Our results indicate that the DLC family members are inefficient GAPs, at least *in vitro*, with catalytic activities that are several orders of magnitude lower than the activities of the RhoGAPs p50 and p190 (Fig. 2*C*) or other highly efficient RhoGAPs, such as GRAF1 or OPHN1 (32).

A comparison of the obtained data on the DLC isoforms with those of other RhoGAP family members raised the question of whether the extremely low GAP activities of DLC proteins stem from effects on either binding affinity (K_d) or catalytic activity (k_{cat}). Therefore, we measured the kinetics of tamraGTP hydrolysis of Cdc42 at increasing concentrations of $DLC1^{GAP}$ and $GRAF1^{GAP}$. The rate constants (k_{obs}) of the fitted single exponential decays increased in a hyperbolic manner as a function of GAP concentrations as described previously (52, 57). We used Cdc42 in most experiments because of a large change in fluorescence upon tamraGTP hydrolysis as compared with Rac1 and RhoA. Fitting a hyperbolic curve to the points according to Equation 1 led to the corresponding kinetic parameters K_d and k_{cat} (Fig. 2*D*).

$$k_{obs} = \frac{k_{cat}}{1 + \frac{K_d}{[DLC1]}} \quad \text{(Eq. 1)}$$

Unlike the relatively similar K_d values, there was a large difference in the k_{cat} values for the GTP hydrolysis reaction: 6.26 s^{-1} for $DLC1^{GAP}$compared with 289 s^{-1} for the highly efficient $GRAF1^{GAP}$. These data clearly indicate that the very low GAP activity of the DLC proteins relies more on the catalytic activity than on the binding affinity to Cdc42.

Insights into cis-Regulatory Modules of DLC1 Function—To examine the influence of other domains of DLC1 (Fig. 1*A*) on its GAP activity, we further measured tamraGTP hydrolysis of Cdc42 stimulated by full-length DLC1 ($DLC1^{fl}$). As shown in Fig. 3*A*, $DLC1^{fl}$ exhibited a strongly reduced GAP activity as compared with the isolated $DLC1^{GAP}$. The k_{obs} values obtained from single turnover kinetic data were 0.02 and 0.47 s^{-1}, respectively, and reveal that the $DLC1^{fl}$ activity was 23.5-fold lower than that of $DLC1^{GAP}$ (Fig. 3*B*). This result strongly supports the previous notion that other regions of DLC1, such as the SAM domain (20), may undergo an intramolecular interaction with the GAP domain and thus contribute to its autoinhibition in a *cis*-inhibitory manner.

To analyze whether the autoinhibitory effect is caused by N- and C-terminal SAM and/or START domains of DLC1 (Fig. 1*A*), we purified these domains and measured their effects on the $DLC1^{GAP}$ activity *in vitro*. Using high concentrations of SAM, START, or both (up to a 100-fold molar excess above the GAP domain), we did not observe any significant inhibition of the $DLC1^{GAP}$ activity using tamraGTP hydrolysis of Cdc42 (Fig. 3*C*). The fact that the isolated SAM and START domains did not reveal any GAP-inhibitory activity strongly suggests that the autoinhibitory mechanism of DLC1 may require additional regions of the full-length protein. One possibility is the serine-rich 14-3-3 binding region between the SAM and the GAP domains (Fig. 1*A*).

p120 SH3 as a Potent trans-Inhibitory Factor of the $DLC1^{GAP}$ Activity—The SH3 domain of p120 has been reported as a novel binding partner of DLC1 with GAP-inhibitory and growth suppression activity (11). To monitor this effect in real time, $DLC1^{GAP}$ activity was measured in the absence and presence of purified $p120^{SH3}$ under the same conditions as in the experiments described above (Fig. 2). As shown in Fig. 4*A*, $DLC1^{GAP}$-

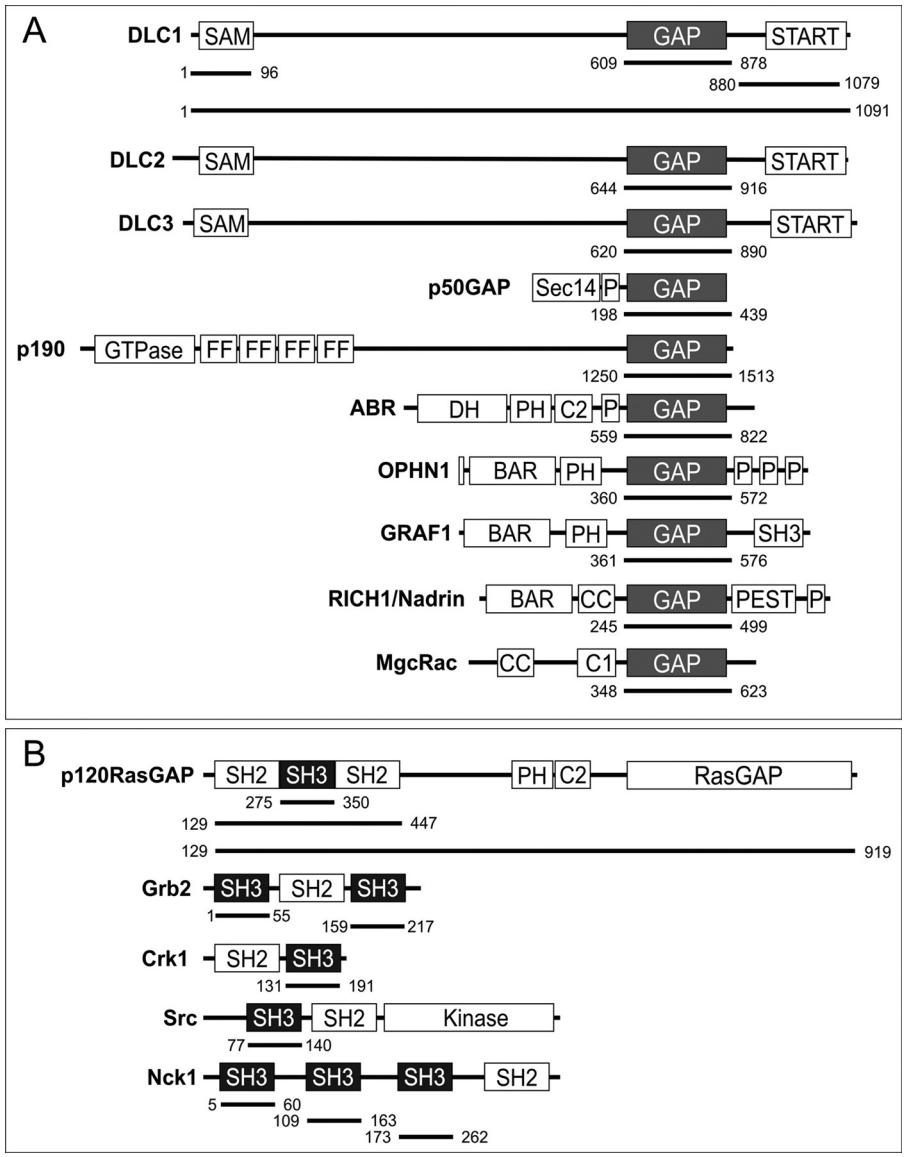

FIGURE 1. **Schematic representation of domain organization and designed fragments of GAP (*A*) and SH3 domain-containing proteins (*B*) used in this study.** The *numbers* indicate the N and C termini of the amino acids of the respective fragments. *BAR*, Bin/Amphiphysin/Rvs; *C1*, cysteine-rich region; *CC*, coiled coil; *DH*, Dbl homology domain; *FF*, double phenylalanine; *P*, proline-rich; *PH*, pleckstrin homology; *PSET*, proline, serine, glutamic acid, and threonine; *RGS*, regulator of G-protein signaling; *Sec14*, secretion and cell surface growth 14.

stimulated tamraGTP hydrolysis of Cdc42 was drastically reduced using a 10-fold excess of $p120^{SH3}$ over the $DLC1^{GAP}$ concentration. The respective k_{obs} value of 0.63 for $DLC1^{GAP}$ activity was reduced by 83-fold in the presence of $p120^{SH3}$ to 0.0076 s^{-1} (Fig. 4*B*), which is close to the intrinsic tamraGTP hydrolysis of Cdc42 (0.02 s^{-1}). These measurements were also performed for RhoA and Rac1 using the same conditions as for Cdc42 (Fig. 4*B*). Similarly, 247- and 15.5-fold reductions of the $DLC1^{GAP}$ activity for RhoA and Rac1, respectively, were determined in the presence of a 10-fold molar excess of $p120^{SH3}$. An explanation for this large variation may be the significant differences in $DLC1^{GAP}$ binding affinity for the three members of the Rho family.

In the next step, we analyzed the inhibitory effect of $p120^{SH3}$ on the GAP activity of DLC2 and DLC3 toward Cdc42. Fig. 4*C* shows that the catalytic GAP activity of purified $DLC2^{GAP}$ and $DLC3^{GAP}$ was also inhibited in the presence of $p120^{SH3}$ but not as drastically as in the case of $DLC1^{GAP}$. The next question we addressed was whether the SH3 domain is freely accessible to exert its inhibitory effect or whether other domains of p120 also play a role in the inhibition of DLC GAP activity (Fig. 1). Therefore, we purified the SH2-SH3-SH2-encompassing $p120^{SH2\text{-}3\text{-}2}$ and N-terminal truncated $p120^{\Delta n128}$ proteins and analyzed their $DLC1^{GAP}$ inhibitory effects in direct comparison with isolated $p120^{SH3}$. Larger p120 fragments inhibited the $DLC1^{GAP}$ activity but to a 19- and 10-fold lower extent than $p120^{SH3}$ (Fig. 4*D*).

Taken together, our *in vitro* data demonstrate that (i) $p120^{SH3}$ acts as a potent *trans*-inhibitory factor of the GAP activity of the DLC isoforms and (ii) the SH3 domain of p120 is not completely unmasked (freely accessible) in the presence of other p120 domains, especially the adjacent SH2 domains. Whether the N-terminal 128 amino acids play a role in this regard remains unclear. Full-length p120 could not be purified due to its instability.

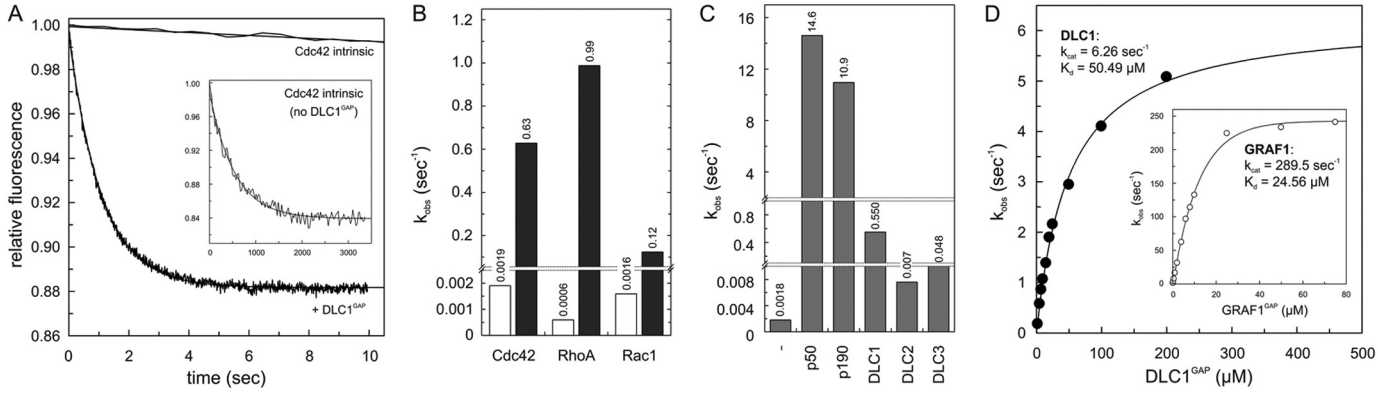

FIGURE 2. **Inefficient GAP activities of the DLC isoforms.** *A*, Cdc42-tamraGTP (0.2 μM) was rapidly mixed with 5 μM DLC1^{GAP} to monitor the GAP-stimulated tamraGTP hydrolysis reaction of Cdc42 in real time. Note the very slow intrinsic GTPase reaction of Cdc42 (*inset*) that was measured in the absence of GAP. Rate constants (k_{obs}) were obtained by single exponential fitting of the data. *B*, the k_{obs} values of GTP hydrolysis of Rho proteins (0.2 μM) measured in the presence of DLC1^{GAP} (5 μM) are represented as a column chart. Calculated -fold activation values were obtained by dividing the k_{obs} values of GAP-stimulated reactions by the k_{obs} values of the intrinsic reactions of respective GTPases. For convenience, the k_{obs} values are given above the *bar charts*. *C*, measured GAP activities of DLC1, DLC2, and DLC3 (5 μM, respectively) toward Cdc42 (0.2 μM) were very low as compared with p150 and p190. *D*, the GTP hydrolysis of Cdc42 (0.2 μM) was measured in the presence of increasing concentrations of the respective GAP domains of DLC1 and GRAF1 (*inset*). The dependence of the k_{obs} values of the GAP-stimulated GTP hydrolysis plotted on the concentrations of DLC1^{GAP} and GRAF1 was fitted by a hyperbolic curve to obtain the kinetic parameters (k_{cat} and K_d).

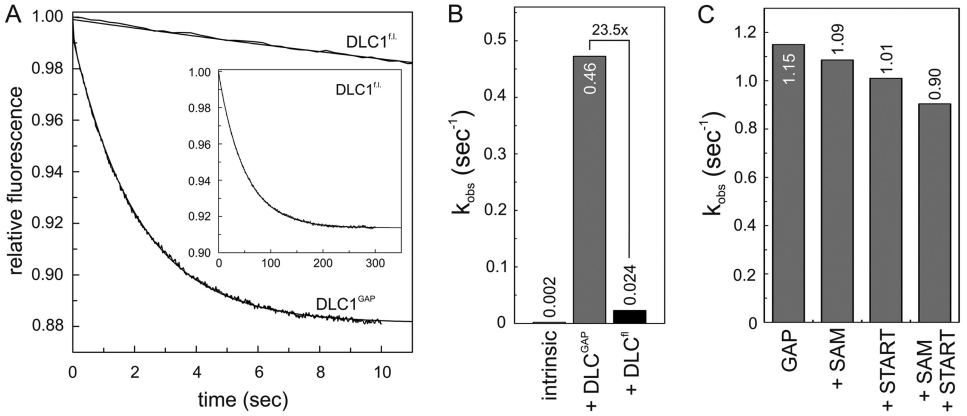

FIGURE 3. ***cis*-Acting regulation of DLC1^{GAP} activity.** *A*, kinetics of the tamraGTP hydrolysis reaction of Cdc42 (0.2 μM) stimulated by DLC1^{fl} (5 μM) was much slower (*inset*) than that stimulated by DLC^{GAP} (5 μM). *B*, the k_{obs} values, illustrated as a bar chart, showed that the GAP activity of DLC1^{fl} is reduced by 23.5-fold as compared with that of the DLC1^{GAP} but not completely inhibited as compared with the intrinsic GTPase reaction. For convenience, the k_{obs} values are given above the *bar charts*. *C*, the activity of DLC1^{GAP} (10 μM) on tamraGTP hydrolysis of Cdc42 (0.2 μM) was not significantly changed in the presence of a 100-fold excess of SAM, START, or both domains (1 mM, respectively).

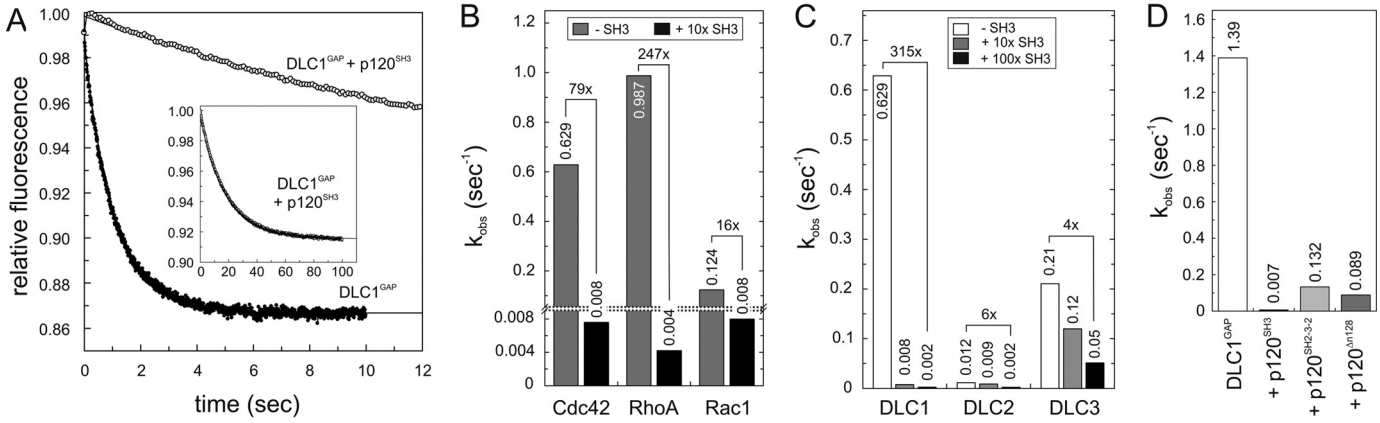

FIGURE 4. **p120^{SH3} as a potent inhibitor of the DLC GAP function.** *A*, kinetics of the tamraGTP hydrolysis reaction of Cdc42 (0.2 μM) stimulated by DLC1^{GAP} (5 μM) was reduced in the presence of a 10-fold excess of p120^{SH3} (50 μM). The complete reaction is shown in the *inset*. *B*, DLC1^{GAP} activities toward Cdc42, RhoA, and Rac1, measured under the same conditions as in *A*, are strongly inhibited by p120^{SH3}. For convenience, the k_{obs} values are given above the *bar charts*. *C*, DLC3^{GAP} (5 μM) was not inhibited by p120^{SH3} (50 and 500 μM) as efficiently as DLC1^{GAP} and DLC2^{GAP} (5 μM, respectively). *D*, p120$^{SH2\text{-}3\text{-}2}$ and p120$^{\Delta n128}$ (40 μM) inhibited the activity of DLC^{GAP} (10 μM) but not as efficiently as p120^{SH3} (40 μM).

Highly Selective Interaction between p120^{SH3} and DLC1^{GAP}—The next issue we addressed was the selectivity of the p120^{SH3} toward DLC1^{GAP}. Therefore, we purified seven additional RhoGAP and SH3 domains of other proteins (Fig. 1). We measured the effect of p120^{SH3} on the GAP activity of Abr, GRAF1, MgcRacGAP, Nadrin, OPHN1, p50, and p190 on the one hand

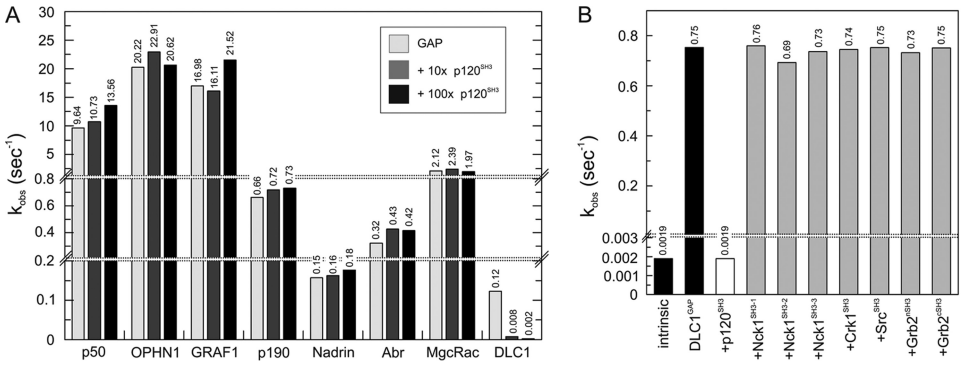

FIGURE 5. **Highly selective interaction between p120^{SH3} and DLC1^{GAP}.** *A*, p120^{SH3}-inhibiting effect on seven additional RhoGAPs (2 μM, respectively) was measured using the tamraGTP hydrolysis reaction of Cdc42 (0.2 μM) and p120^{SH3} (20 and 200 μM, respectively). p120^{SH3} inhibited only DLC1^{GAP} but not the other RhoGAPs. For convenience, the k_{obs} values are given above the *bar charts*. *B*, the effect of seven additional SH3 proteins (100 μM, respectively) on inhibiting DLC1^{GAP} (10 μM) was measured. Only p120^{SH3} inhibited DLC1^{GAP} but not the other SH3 domains.

and the effects of the SH3 domains of Crk1, c-Src, Grb2 (N- and C-terminal SH3 domains), and Nck1 (all three SH3 domains) on the DLC1^{GAP} activity on the other hand. As summarized in Fig. 5, neither did p120^{SH3} inhibit the activity of other GAPs of the Rho family (Fig. 5*A*) nor was the DLC1^{GAP} activity affected by the presence of other SH3 domains (Fig. 5*B*). These data clearly demonstrate that the p120^{SH3}-mediated *trans*-inhibition of DLC isoforms is highly selective.

Potent DLC1 Inhibition Due to High Affinity p120^{SH3}-DLC1^{GAP} Complex Formation—In the next step, we characterized in more detail the interaction between p120^{SH3} and DLC1^{GAP} as well as the inhibition of the DLC1^{GAP} activity induced by p120^{SH3} using different qualitative and quantitative biophysical and biochemical methods. aSEC is an accurate and simple method to visualize high affinity protein-protein interactions. p120^{SH3} (9 kDa) and DLC1^{GAP} (31 kDa) alone and a mixture of both proteins were loaded on a Superdex 75 (10/300) column, and eluted peak fractions were analyzed by SDS-PAGE. Data summarized in Fig. 6*A* clearly illustrate that a mixture of p120^{SH3} and DLC1^{GAP} shift the elution profile of the respective protein domains to an elution volume of 10.5 ml, indicating the formation of a complex between both proteins. We next determined the inhibitory potency of p120^{SH3} by measuring DLC1^{GAP} activity at increasing concentrations of p120^{SH3}. An inhibitory constant (K_i) of 0.61 μM was calculated by fitting the Morrison equation for a tight binding inhibitor (58) to individual k_{obs} values plotted against different p120^{SH3} concentrations (Fig. 6*B*). Furthermore, we measured the dissociation constant of the p120^{SH3}-DLC1^{GAP} interaction using ITC. The results shown in Fig. 6*C* allowed the determination of a stoichiometry of 1:1 and a dissociation constant (K_d) of 0.6 μM for the binding of p120^{SH3} to DLC1^{GAP} (Fig. 6*C*); this value nicely resembles the K_i value obtained from inhibition kinetics (Fig. 6*B*). This binding affinity is remarkably high and unexpected considering the low micromolar range affinities of SH3 domains for their P*XX*P-containing proteins (59). Taken together, these data strongly suggest that the mode of the p120^{SH3}-DLC1^{GAP} interaction most likely differs from the conventional SH3 interaction with P*XX*P loop motifs as recently published (48).

Structural Insight into a Putative Binding Mode between p120^{SH3} and DLC1^{GAP}—The high nanomolar affinity of p120^{SH3} for DLC1^{GAP} and the absence of a P*XX*P motif in DLC1^{GAP} strongly support the notion that the p120^{SH3}-DLC1^{GAP} interaction is mediated via a novel binding mechanism. To gain insight into the structural basis of this interaction, we first performed protein-protein docking of available crystal structures of p120^{SH3} (Protein Data Bank code 2J05) (53) and DLC1^{GAP} (Protein Data Bank code 3KUQ) using the PatchDock program (54). The model of the complex ranked as the first among 20 resulting models fulfilled the criteria for a close proximity of p120^{SH3} to the catalytic arginine finger (Arg-677) of the DLC1^{GAP} domain and was thus selected for refinement by molecular modeling methods. Inspecting the refined model, we identified three potential DLC1^{GAP} binding residues of p120^{SH3} (Asn-311, Leu-313, and Trp-319) that were closest to the catalytic Arg-677 of DLC1^{GAP} (Fig. 7*A*). We proposed that mutation of these residues may impair binding of the SH3 domain, which otherwise masks the arginine finger of DLC1^{GAP}. Catalytic arginine is known to stabilize the transition intermediate state of the hydrolysis reaction in the active center of Rho proteins (Fig. 7*B*) (14, 60). This assumption also suggests that p120 competitively inhibits DLC1 GAP function.

To validate our assumption, we performed mutational analysis of the above mentioned key residues at the p120^{SH3}-DLC1^{GAP} interface: N311R, L313A, and W319G in p120^{SH3} (single, double, and triple single point mutations) and R677A in DLC1^{GAP}. Expectedly, DLC1^{GAP} with the catalytic arginine finger substituted to alanine was deficient in stimulating tamraGTP hydrolysis of Cdc42 (data not shown) and most remarkably in associating with p120^{SH3} (Fig. 8, *A* and *B*). The latter was examined using two independent methods, ITC and aSEC. Reciprocally, p120$^{SH3(N311R,L313A,W319G)}$ was almost disabled in inhibiting DLC1^{GAP} activity (Fig. 8*E*), most probably due to its inability to bind to DLC1^{GAP} (Fig. 8, *C* and *D*). The analysis of the single point mutations revealed that W319G substitution had a minor effect on the association with (data not shown) and on the inhibition of DLC^{GAP} (Fig. 8*E*). p120$^{SH3(N311R,L313A)}$ on the other hand significantly abolished both the inhibitory effect of p120^{SH3} (Fig. 8*E*) and the complex formation with DLC1^{GAP} (data not shown) as compared with wild-type p120^{SH3}. Taken together,

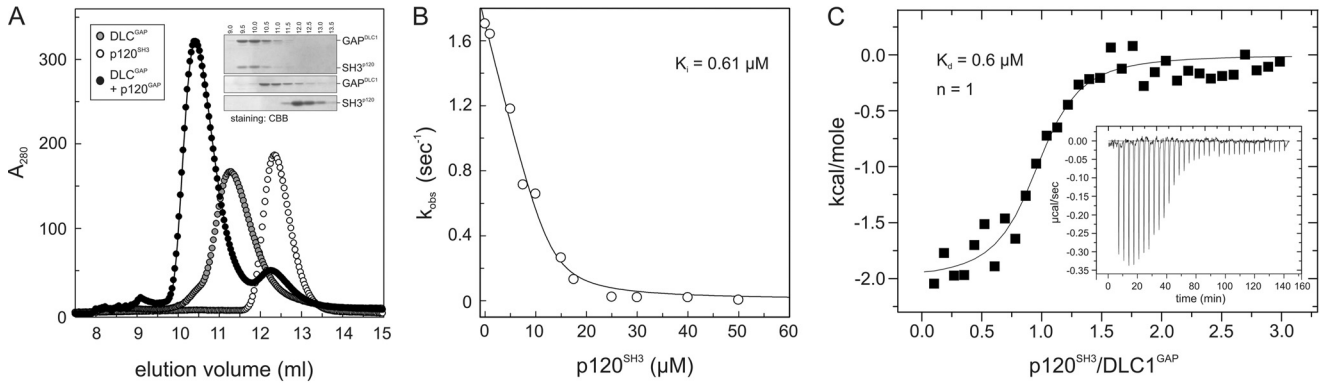

FIGURE 6. **High affinity interaction between p120^{SH3} and DLC1^{GAP}.** *A*, co-elution of a mixture of DLC1^{GAP} (10 μM) and p120^{SH3} (15 μM) (*open circles*) from a Superdex 75 (10/300) as shown by SDS-PAGE (15%) and Coomassie Brilliant Blue (*CBB*) staining (*inset*) indicates their complex formation. *B*, the activity of DLC1^{GAP} (20 μM) toward Cdc42 (0.2 μM) was measured at increasing concentrations of p120^{SH3}, and the obtained k_{obs} values were plotted against increasing concentrations of the inhibitor p120^{SH3}. The K_i value was obtained by non-linear regression based on the Morrison equation for tight binding inhibitors (58). *C*, ITC analysis was performed by titrating DLC1^{GAP} (20 μM) with p120^{SH3} (400 μM). K_d is the dissociation constant, and *n* is the stoichiometry.

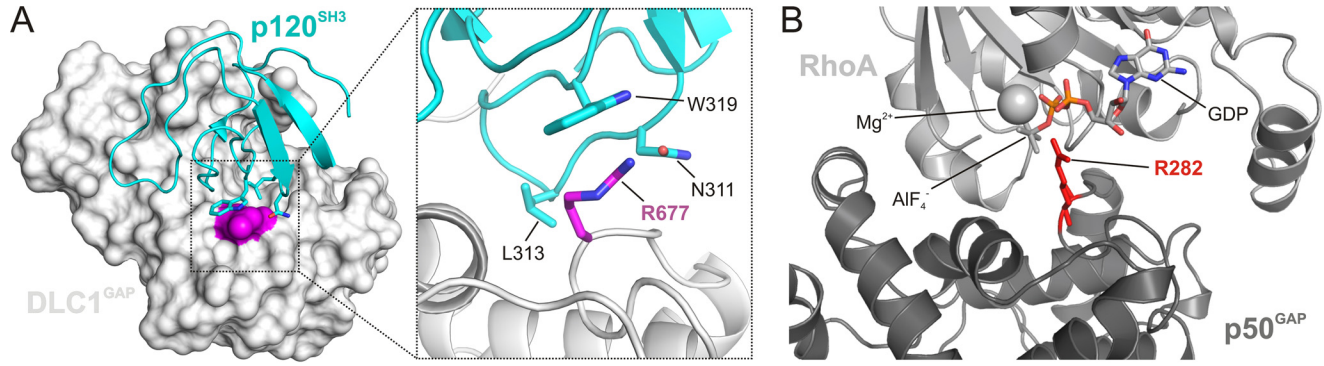

FIGURE 7. **Structural insight into a putative binding mode between p120^{SH3} and DLC1^{GAP}.** *A*, molecular docking analyses were performed between the available crystal structures of p120^{SH3} (Protein Data Bank code 2J05) (53) and DLC1^{GAP} (Protein Data Bank code 3KUQ) using the program PatchDock (54). In the best ranked and refined model, p120^{SH3} was located in close proximity of the catalytic arginine finger (Arg-677; *magenta*) of DLC1^{GAP}. In this model, p120^{SH3} supplied three amino acids (Asn-311, Leu-313, and Trp-319) to directly contact the catalytic core of DLC1^{GAP}, especially Arg-677, and mask its accessibility to the Rho proteins. *B*, p50GAP provides an arginine finger (Arg-282; *red*) in the active site of RhoA to stabilize the transition state of the GTP hydrolysis reaction (Protein Data Bank code 1TX4) (60). GDP-AlF_4^- mimics the transition state of the GTP hydrolysis reaction.

our mutational and biochemical analyses support the *in silico* structural model (Fig. 7*A*) and provide new insight into how p120^{SH3} may bind and inhibit the catalytic activity of DLC1^{GAP}.

DISCUSSION

In this study, we have elucidated the molecular mechanism of how the RasGAP p120 selectively acts as a negative regulator of the RhoGAP activity of DLC1. We have shown that p120^{SH3}, by utilizing a novel binding mode, selectively undergoes a high affinity interaction with the RhoGAP domain of DLC1 and effectively inhibits its GAP activity by targeting its catalytic arginine finger. Interestingly, p120^{SH3} acts on the DLC isoforms but not on seven other representative members of the RhoGAP family. Our data together support the notion of a functional cross-talk between Ras and Rho proteins at the level of regulatory proteins (11, 45).

In contrast to the molecular mechanism of Rho protein inactivation by GAPs, which is well established (14, 61), it is still unclear how GAPs themselves are regulated. Different mechanisms are implicated in the regulation of GAPs, such as regulation by protein phosphorylation, proteolytic degradation, intramolecular autoinhibition, and changes in subcellular localization or protein complex formation (62, 63). "Intramolecular inhibition" (also called "autoinhibition," "*cis*-inhibition," "autoinhibitory loop," "autoregulation," and "bistable switch") of biological molecules is a fundamental control mechanism in nature and is an emerging theme in the regulation of different kinds of proteins, including the regulators of small GTP-binding proteins themselves. Besides the guanine nucleotide exchange factors (64–69), GAPs also have been reported to require activation through the relief of autoinhibitory elements (20, 31–33, 35, 36). Kim *et al.* (20) have shown that DLC1^{fl} has a reduced GAP activity and have proposed that the N-terminal SAM domain may be a *cis*-inhibitory element contributing to DLC1 autoinhibition. Our real time kinetic experiments, however, have shown that neither isolated SAM or START alone nor both domains in combination are directly responsible for the observed DLC1^{fl} autoinhibition in a cell-free system (Fig. 3). Taken together, it rather seems plausible that other regions, probably together with SAM and START domains, are involved in the autoinhibition of DLC1. In addition, it is important to note that release of the autoinhibitory loop of DLC1 is most likely subjected to posttranslational modifications (21, 70) and interactions with other proteins (16, 28, 34) along with changes in subcellular localization (30), collectively contribute to the regulation of DLC1 GAP activity in intact cells. In this context, PKD-mediated phosphorylation (70) and 14-3-3 binding and

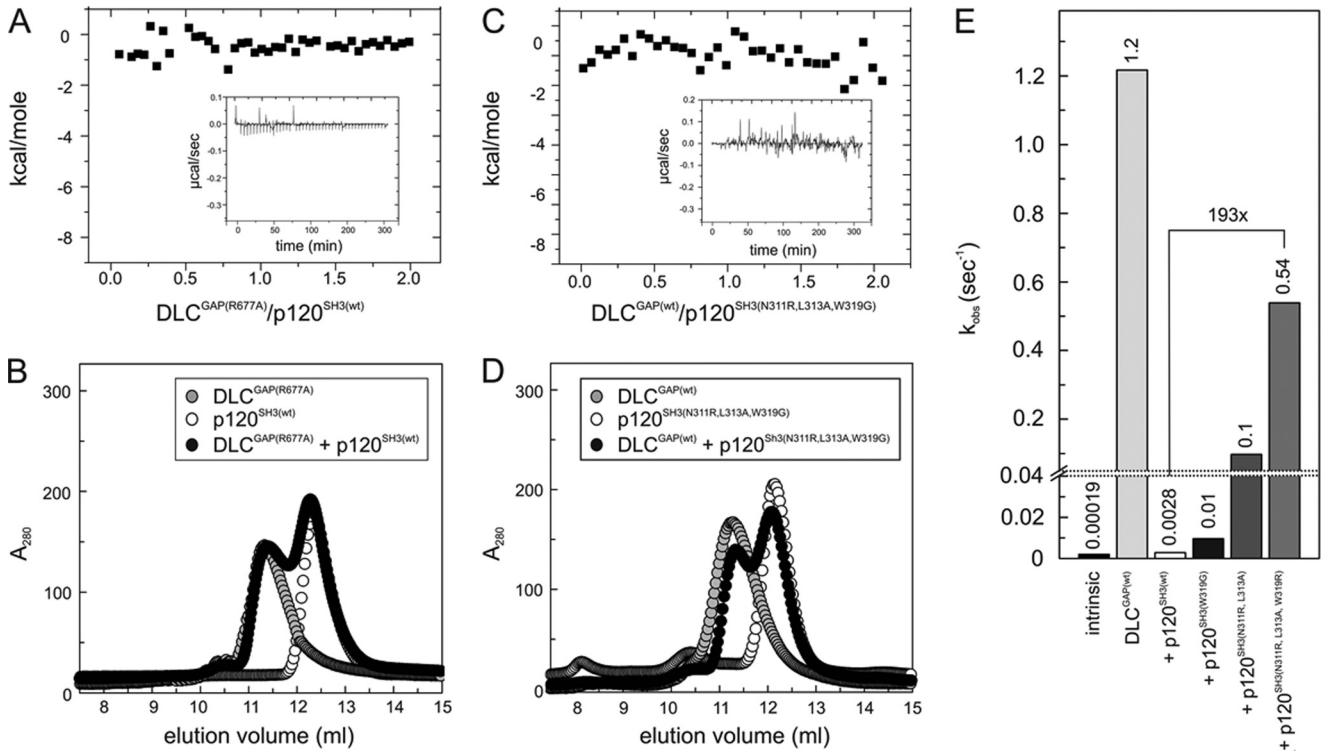

FIGURE 8. **Loss of p120-DLC1 interaction by mutational analysis.** No interaction was observed between DLC1$^{GAP(R677A)}$ and p120$^{SH3(WT)}$ (*A* and *B*) and DLC1$^{GAP(WT)}$ and p120$^{SH3(N311R,L313A,W319G)}$ (*C* and *D*). Loss of interaction and of inhibition was measured by ITC (*A* and *C*) and aSEC (*B* and *D*) as compared with the p120$^{SH3(WT)}$-DLC1$^{GAP(WT)}$ interaction shown in Fig. 6. *E*, the activity of DLC1^{GAP} (25 μM) in stimulating tamraGTP hydrolysis of Cdc42 (0.2 μM) was measured in the presence of p120^{SH3} variants (125 μM), respectively. For convenience, the k_{obs} values are given above the *bar charts*.

cytosolic sequestration (22) are good examples for the regulation DLC1 function.

Functional characterization and structural elucidation of the *trans*-inhibitory mechanism of DLC1 mediated by the Ras-specific GAP p120 protein (11) was the central theme of this study. Our data clearly revealed that the GAP activity of not only DLC1 but also that of DLC2 and DLC3 was almost completely abolished in the presence of the SH3 domain of p120 (Fig. 4). We showed that larger fragments of p120, such as p120$^{SH2\text{-}3\text{-}2}$ and the almost full-length p120$^{\Delta n128}$, inhibit the DLC GAP function but strikingly not to the same extent as seen for the isolated SH3 domain (Fig. 4*D*). These data indicate that only a freely accessible and exposed SH3 domain of p120, most probably following an upstream signal and in a defined subcellular environment (11, 37), is able to potently inhibit DLC proteins. One of the p120 binding partners is p190, which has been proposed to induce a conformational change in p120 by binding to its SH2 domains and exposing the adjacent SH3 domain for additional protein interactions with additional proteins (47), one of which is most likely DLC1.

Several studies have shown that DLC1 is able to inactivate Cdc42 and the Rho isoforms (RhoA, RhoB, and RhoC) but not Rac1 *in vitro* (20, 71–73). DLC1^{GAP} activity toward other members of the Rho family has not yet been published. Our preliminary data showed that the DLC proteins are active *in vitro* on almost all members of the Rho family that are able to hydrolyze GTP.[6]

Chan *et al.* (74) have shown an increased level of RhoA-GTP in DLC2-null mice but not in samples from control mice. Consistently, the overexpression of DLC isoforms has been shown to lead to inactivation of RhoA and to the reduction of actin stress fiber formation (75, 76), suggesting that DLC proteins are Rho-selective GAPs and the role of the DLC *trans*-inhibitory protein p120 is to retain Rho proteins in their active GTP-bound states. Contrary to DLC proteins, p120 binding is part of the p190 activation process that controls inactivation of Rho-type proteins (45, 47, 77). A prerequisite for this interaction is phosphorylation of p190 at tyrosine 1105, which is a target of the p120 SH2 domains (77). In this regard, p120 oppositely controls the activities of two different RhoGAPs and obviously two different Rho/Rho effector systems; one is left activated, and the other is switched off.

SH3 domain-containing cellular signaling proteins mediate interactions via specific proline-containing peptides. The SH3 domain of p120 has been discussed recently to interact with other proteins in a P*XX*P motif-independent manner (48). *In silico* analysis revealed that the GAP domain of DLC1 does not possess a proline-rich region and therefore, unlike classical P*XX*P motif-recognizing SH3 domains, the interaction mode of the p120 SH3 domain is atypical and utilizes different amino acids to bind and mask the catalytic arginine finger of the GAP domain of DLC1. The Ser/Thr kinases Aurora A and Aurora B are other examples in addition to DLC1 for negative modulation of biological processes by p120 (78). The SH3 domain of p120 binds to the catalytic domain of Aurora kinases that inhibits their kinase activity. These interactions also do not involve a

[6] M. Jaiswal, E. Amin, and R. Dvorsky, unpublished data.

proline-rich consensus sequence. Two accessible hydrophobic regions of p120 SH3 have been suggested to function as binding sites for protein interaction (79). Our study supports this notion as we have shown that mutation of three amino acids close to one of these proposed binding sites indeed diminished the $DLC1^{GAP}$ binding and inhibiting ability of p120 SH3.

We demonstrated that the interaction between $p120^{SH3}$ and $DLC1^{GAP}$ displays at least three remarkable characteristics, namely high affinity, high selectively, and a non-canonical binding mode. The high affinity interaction of 0.6 μM is striking because the binding constants of SH3 domains for proline-rich motifs in their target proteins are mostly in the micromolar range (48, 59). The very few examples of high affinity binding of SH3 domains are those between Mona/Gads and SLP-76 (80), C3G and c-Crk (51), and Grb2 and Wrch1 (48).

CONCLUSION

Mechanistic and structural insights into selectivity, activity, and regulation of DLC1 presented in this study shed light on the role of the multifunctional, regulatory signaling molecule p120RasGAP. It is evident that p120 acts in addition to its RasGAP domain, which is required to switch off Ras signal transduction, as an "effector" conversely controlling, via its SH2 domains and a non-canonical SH3 domain, the RhoGAP activities of the DLC and p190 proteins and hence Rho signal transduction. Interestingly, p120 interacts, in addition to DLC1 and p190, with a third RhoGAP, called p200RhoGAP. In contrast to p190 and DLC1, which are downstream of p120, p200RhoGAP has been proposed to bind to the p120 SH3 domain via its very C-terminal proline-rich region and to sequestrate its RasGAP function from inactivating Ras (10). These examples nicely illustrate the interdependence of the Ras and Rho signaling pathways and underline the multifunctional and multifaceted nature of regulatory proteins beyond their critical GAP functions.

Acknowledgments—We thank Linda van Aelst, Katrin Rittinger, Olivier Dorseui, Gerard Gacon, Alan Hall, Tony Pawson, and Jeffrey Settleman for sharing reagents with us that proved indispensable for the work.

REFERENCES

1. Aznar, S., and Lacal, J. C. (2001) Searching new targets for anticancer drug design: the families of Ras and Rho GTPases and their effectors. *Prog. Nucleic Acid Res. Mol. Biol.* **67,** 193–234
2. Fritz, G., Just, I., and Kaina, B. (1999) Rho GTPases are over-expressed in human tumors. *Int. J. Cancer* **81,** 682–687
3. Pruitt, K., and Der, C. J. (2001) Ras and Rho regulation of the cell cycle and oncogenesis. *Cancer Lett.* **171,** 1–10
4. Zondag, G. C., Evers, E. E., ten Klooster, J. P., Janssen, L., van der Kammen, R. A., and Collard, J. G. (2000) Oncogenic Ras downregulates Rac activity, which leads to increased Rho activity and epithelial-mesenchymal transition. *J. Cell Biol.* **149,** 775–782
5. Sahai, E., and Marshall, C. J. (2002) RHO-GTPases and cancer. *Nat. Rev. Cancer* **2,** 133–142
6. Khosravi-Far, R., Campbell, S., Rossman, K. L., and Der, C. J. (1998) Increasing complexity of Ras signal transduction: involvement of Rho family proteins. *Adv. Cancer Res.* **72,** 57–107
7. Coleman, M. L., Marshall, C. J., and Olson, M. F. (2004) RAS and RHO GTPases in G1-phase cell-cycle regulation. *Nat. Rev. Mol. Cell Biol.* **5,** 355–366
8. Karnoub, A. E., and Weinberg, R. A. (2008) Ras oncogenes: split personalities. *Nat. Rev. Mol. Cell Biol.* **9,** 517–531
9. Asnaghi, L., Vass, W. C., Quadri, R., Day, P. M., Qian, X., Braverman, R., Papageorge, A. G., and Lowy, D. R. (2010) E-cadherin negatively regulates neoplastic growth in non-small cell lung cancer: role of Rho GTPases. *Oncogene* **29,** 2760–2771
10. Shang, X., Moon, S. Y., and Zheng, Y. (2007) p200 RhoGAP promotes cell proliferation by mediating cross-talk between Ras and Rho signaling pathways. *J. Biol. Chem.* **282,** 8801–8811
11. Yang, X. Y., Guan, M., Vigil, D., Der, C. J., Lowy, D. R., and Popescu, N. C. (2009) p120Ras-GAP binds the DLC1 Rho-GAP tumor suppressor protein and inhibits its RhoA GTPase and growth-suppressing activities. *Oncogene* **28,** 1401–1409
12. Scheffzek, K., and Ahmadian, M. R. (2005) GTPase activating proteins: structural and functional insights 18 years after discovery. *Cell. Mol. Life Sci.* **62,** 3014–3038
13. Ligeti, E., Welti, S., and Scheffzek, K. (2012) Inhibition and termination of physiological responses by GTPase activating proteins. *Physiol. Rev.* **92,** 237–272
14. Scheffzek, K., Ahmadian, M. R., and Wittinghofer, A. (1998) GTPase-activating proteins: helping hands to complement an active site. *Trends Biochem. Sci.* **23,** 257–262
15. Yuan, B. Z., Miller, M. J., Keck, C. L., Zimonjic, D. B., Thorgeirsson, S. S., and Popescu, N. C. (1998) Cloning, characterization, and chromosomal localization of a gene frequently deleted in human liver cancer (DLC-1) homologous to rat RhoGAP. *Cancer Res.* **58,** 2196–2199
16. Durkin, M. E., Yuan, B. Z., Zhou, X., Zimonjic, D. B., Lowy, D. R., Thorgeirsson, S. S., and Popescu, N. C. (2007) DLC-1: a Rho GTPase-activating protein and tumour suppressor. *J. Cell. Mol. Med.* **11,** 1185–1207
17. Liao, Y. C., and Lo, S. H. (2008) Deleted in liver cancer-1 (DLC-1): a tumor suppressor not just for liver. *Int. J. Biochem. Cell Biol.* **40,** 843–847
18. Zimonjic, D. B., and Popescu, N. C. (2012) Role of DLC1 tumor suppressor gene and MYC oncogene in pathogenesis of human hepatocellular carcinoma: potential prospects for combined targeted therapeutics (review). *Int. J. Oncol.* **41,** 393–406
19. Holeiter, G., Heering, J., Erlmann, P., Schmid, S., Jähne, R., and Olayioye, M. A. (2008) Deleted in liver cancer 1 controls cell migration through a Dia1-dependent signaling pathway. *Cancer Res.* **68,** 8743–8751
20. Kim, T. Y., Healy, K. D., Der, C. J., Sciaky, N., Bang, Y. J., and Juliano, R. L. (2008) Effects of structure of Rho GTPase-activating protein DLC-1 on cell morphology and migration. *J. Biol. Chem.* **283,** 32762–32770
21. Kim, T. Y., Vigil, D., Der, C. J., and Juliano, R. L. (2009) Role of DLC-1, a tumor suppressor protein with RhoGAP activity, in regulation of the cytoskeleton and cell motility. *Cancer Metastasis Rev.* **28,** 77–83
22. Scholz, R. P., Regner, J., Theil, A., Erlmann, P., Holeiter, G., Jähne, R., Schmid, S., Hausser, A., and Olayioye, M. A. (2009) DLC1 interacts with 14-3-3 proteins to inhibit RhoGAP activity and block nucleocytoplasmic shuttling. *J. Cell Sci.* **122,** 92–102
23. Lukasik, D., Wilczek, E., Wasiutynski, A., and Gornicka, B. (2011) Deleted in liver cancer protein family in human malignancies (review). *Oncol. Lett.* **2,** 763–768
24. Yam, J. W., Ko, F. C., Chan, C. Y., Jin, D. Y., and Ng, I. O. (2006) Interaction of deleted in liver cancer 1 with tensin2 in caveolae and implications in tumor suppression. *Cancer Res.* **66,** 8367–8372
25. Liao, Y. C., Si, L., deVere White, R. W., and Lo, S. H. (2007) The phosphotyrosine-independent interaction of DLC-1 and the SH2 domain of cten regulates focal adhesion localization and growth suppression activity of DLC-1. *J. Cell Biol.* **176,** 43–49
26. Qian, X., Li, G., Asmussen, H. K., Asnaghi, L., Vass, W. C., Braverman, R., Yamada, K. M., Popescu, N. C., Papageorge, A. G., and Lowy, D. R. (2007) Oncogenic inhibition by a deleted in liver cancer gene requires cooperation between tensin binding and Rho-specific GTPase-activating protein activities. *Proc. Natl. Acad. Sci. U.S.A.* **104,** 9012–9017
27. Chan, L. K., Ko, F. C., Ng, I. O., and Yam, J. W. (2009) Deleted in liver cancer 1 (DLC1) utilizes a novel binding site for Tensin2 PTB domain interaction and is required for tumor-suppressive function. *PLoS One* **4,** e5572

28. Tripathi, V., Popescu, N. C., and Zimonjic, D. B. (2013) DLC1 induces expression of E-cadherin in prostate cancer cells through Rho pathway and suppresses invasion. *Oncogene* **4,** 1–10
29. Li, G., Du, X., Vass, W. C., Papageorge, A. G., Lowy, D. R., and Qian, X. (2011) Full activity of the deleted in liver cancer 1 (DLC1) tumor suppressor depends on an LD-like motif that binds talin and focal adhesion kinase (FAK). *Proc. Natl. Acad. Sci. U.S.A.* **108,** 17129–17134
30. Erlmann, P., Schmid, S., Horenkamp, F. A., Geyer, M., Pomorski, T. G., and Olayioye, M. A. (2009) DLC1 activation requires lipid interaction through a polybasic region preceding the RhoGAP domain. *Mol. Biol. Cell* **20,** 4400–4411
31. Fauchereau, F., Herbrand, U., Chafey, P., Eberth, A., Koulakoff, A., Vinet, M. C., Ahmadian, M. R., Chelly, J., and Billuart, P. (2003) The RhoGAP activity of OPHN1, a new F-actin-binding protein, is negatively controlled by its amino-terminal domain. *Mol. Cell. Neurosci.* **23,** 574–586
32. Eberth, A., and Ahmadian, M. R. (2009) *In vitro* GEF and GAP assays. *Curr. Protoc. Cell Biol.* **Chapter 14,** Unit 14.19
33. Colón-González, F., Leskow, F. C., and Kazanietz, M. G. (2008) Identification of an autoinhibitory mechanism that restricts C1 domain-mediated activation of the Rac-GAP α2-chimaerin. *J. Biol. Chem.* **283,** 35247–35257
34. Jian, X., Brown, P., Schuck, P., Gruschus, J. M., Balbo, A., Hinshaw, J. E., and Randazzo, P. A. (2009) Autoinhibition of Arf GTPase-activating protein activity by the BAR domain in ASAP1. *J. Biol. Chem.* **284,** 1652–1663
35. Zhou, Y. T., Chew, L. L., Lin, S. C., and Low, B. C. (2010) The BNIP-2 and Cdc42GAP homology (BCH) domain of p50RhoGAP/Cdc42GAP sequesters RhoA from inactivation by the adjacent GTPase-activating protein domain. *Mol. Biol. Cell* **21,** 3232–3246
36. Moskwa, P., Paclet, M. H., Dagher, M. C., and Ligeti, E. (2005) Autoinhibition of p50 Rho GTPase-activating protein (GAP) is released by prenylated small GTPases. *J. Biol. Chem.* **280,** 6716–6720
37. Pamonsinlapatham, P., Hadj-Slimane, R., Lepelletier, Y., Allain, B., Toccafondi, M., Garbay, C., and Raynaud, F. (2009) p120-Ras GTPase activating protein (RasGAP): a multi-interacting protein in downstream signaling. *Biochimie* **91,** 320–328
38. Ahmadian, M. R., Hoffmann, U., Goody, R. S., and Wittinghofer, A. (1997) Individual rate constants for the interaction of Ras proteins with GTPase-activating proteins determined by fluorescence spectroscopy. *Biochemistry* **36,** 4535–4541
39. Ahmadian, M. R., Stege, P., Scheffzek, K., and Wittinghofer, A. (1997) Confirmation of the arginine-finger hypothesis for the GAP-stimulated GTP-hydrolysis reaction of Ras. *Nat. Struct. Biol.* **4,** 686–689
40. Scheffzek, K., Ahmadian, M. R., Kabsch, W., Wiesmüller, L., Lautwein, A., Schmitz, F., and Wittinghofer, A. (1997) The Ras-RasGAP complex: structural basis for GTPase activation and its loss in oncogenic Ras mutants. *Science* **277,** 333–338
41. Leblanc, V., Tocque, B., and Delumeau, I. (1998) Ras-GAP controls Rho-mediated cytoskeletal reorganization through its SH3 domain. *Mol. Cell. Biol.* **18,** 5567–5578
42. Chan, P. C., and Chen, H. C. (2012) p120RasGAP-mediated activation of c-Src is critical for oncogenic Ras to induce tumor invasion. *Cancer Res.* **72,** 2405–2415
43. Clark, G. J., and Der, C. J. (1995) Aberrant function of the Ras signal transduction pathway in human breast cancer. *Breast Cancer Res. Treat.* **35,** 133–144
44. Clark, G. J., Westwick, J. K., and Der, C. J. (1997) p120 GAP modulates Ras activation of Jun kinases and transformation. *J. Biol. Chem.* **272,** 1677–1681
45. Herbrand, U., and Ahmadian, M. R. (2006) p190-RhoGAP as an integral component of the Tiam1/Rac1-induced downregulation of Rho. *Biol. Chem.* **387,** 311–317
46. Wang, Z., Tung, P. S., and Moran, M. F. (1996) Association of p120 ras GAP with endocytic components and colocalization with epidermal growth factor (EGF) receptor in response to EGF stimulation. *Cell Growth Differ.* **7,** 123–133
47. Hu, K. Q., and Settleman, J. (1997) Tandem SH2 binding sites mediate the RasGAP-RhoGAP interaction: a conformational mechanism for SH3 domain regulation. *EMBO J.* **16,** 473–483
48. Risse, S. L., Vaz, B., Burton, M. F., Aspenström, P., Piekorz, R. P., Brunsveld, L., and Ahmadian, M. R. (2013) SH3-mediated targeting of Wrch1/RhoU by multiple adaptor proteins. *Biol. Chem.* **394,** 421–432
49. Jaiswal, M., Dubey, B. N., Koessmeier, K. T., Gremer, L., and Ahmadian, M. R. (2012) Biochemical assays to characterize Rho GTPases. *Methods Mol. Biol.* **827,** 37–58
50. Eberth, A., Lundmark, R., Gremer, L., Dvorsky, R., Koessmeier, K. T., McMahon, H. T., and Ahmadian, M. R. (2009) A BAR domain-mediated autoinhibitory mechanism for RhoGAPs of the GRAF family. *Biochem. J.* **417,** 371–377
51. Wu, X., Knudsen, B., Feller, S. M., Zheng, J., Sali, A., Cowburn, D., Hanafusa, H., and Kuriyan, J. (1995) Structural basis for the specific interaction of lysine-containing proline-rich peptides with the N-terminal SH3 domain of c-Crk. *Structure* **3,** 215–226
52. Eberth, A., Dvorsky, R., Becker, C. F., Beste, A., Goody, R. S., and Ahmadian, M. R. (2005) Monitoring the real-time kinetics of the hydrolysis reaction of guanine nucleotide-binding proteins. *Biol. Chem.* **386,** 1105–1114
53. Ross, B., Kristensen, O., Favre, D., Walicki, J., Kastrup, J. S., Widmann, C., and Gajhede, M. (2007) High resolution crystal structures of the p120 RasGAP SH3 domain. *Biochem. Biophys. Res. Commun.* **353,** 463–468
54. Schneidman-Duhovny, D., Inbar, Y., Nussinov, R., and Wolfson, H. J. (2005) PatchDock and SymmDock: servers for rigid and symmetric docking. *Nucleic Acids Res.* **33,** W363–W367
55. Brooks, B. R., Brooks, C. L., 3rd, Mackerell, A. D., Jr., Nilsson, L., Petrella, R. J., Roux, B., Won, Y., Archontis, G., Bartels, C., Boresch, S., Caflisch, A., Caves, L., Cui, Q., Dinner, A. R., Feig, M., Fischer, S., Gao, J., Hodoscek, M., Im, W., Kuczera, K., Lazaridis, T., Ma, J., Ovchinnikov, V., Paci, E., Pastor, R. W., Post, C. B., Pu, J. Z., Schaefer, M., Tidor, B., Venable, R. M., Woodcock, H. L., Wu, X., Yang, W., York, D. M., and Karplus, M. (2009) CHARMM: the biomolecular simulation program. *J. Comput. Chem.* **30,** 1545–1614
56. Scouras, A. D., and Daggett, V. (2011) The Dynameomics rotamer library: amino acid side chain conformations and dynamics from comprehensive molecular dynamics simulations in water. *Protein Sci.* **20,** 341–352
57. Eccleston, J. F., Moore, K. J., Morgan, L., Skinner, R. H., and Lowe, P. N. (1993) Kinetics of interaction between normal and proline 12 Ras and the GTPase-activating proteins, p120-GAP and neurofibromin. The significance of the intrinsic GTPase rate in determining the transforming ability of *ras*. *J. Biol. Chem.* **268,** 27012–27019
58. Morrison, J. F. (1969) Kinetics of the reversible inhibition of enzyme-catalysed reactions by tight-binding inhibitors. *Biochim. Biophys. Acta* **185,** 269–286
59. Kärkkäinen, S., Hiipakka, M., Wang, J. H., Kleino, I., Vähä-Jaakkola, M., Renkema, G. H., Liss, M., Wagner, R., and Saksela, K. (2006) Identification of preferred protein interactions by phage-display of the human Src homology-3 proteome. *EMBO Rep.* **7,** 186–191
60. Rittinger, K., Walker, P. A., Eccleston, J. F., Smerdon, S. J., and Gamblin, S. J. (1997) Structure at 1.65 Å of RhoA and its GTPase-activating protein in complex with a transition-state analogue. *Nature* **389,** 758–762
61. Dvorsky, R., and Ahmadian, M. R. (2004) Always look on the bright site of Rho: structural implications for a conserved intermolecular interface. *EMBO Rep.* **5,** 1130–1136
62. Moon, S. Y., and Zheng, Y. (2003) Rho GTPase-activating proteins in cell regulation. *Trends Cell Biol.* **13,** 13–22
63. Tcherkezian, J., and Lamarche-Vane, N. (2007) Current knowledge of the large RhoGAP family of proteins. *Biol. Cell* **99,** 67–86
64. Rossman, K. L., Der, C. J., and Sondek, J. (2005) GEF means go: turning on RHO GTPases with guanine nucleotide-exchange factors. *Nat. Rev. Mol. Cell Biol.* **6,** 167–180
65. Aittaleb, M., Boguth, C. A., and Tesmer, J. J. (2010) Structure and function of heterotrimeric G protein-regulated Rho guanine nucleotide exchange factors. *Mol. Pharmacol.* **77,** 111–125
66. DiNitto, J. P., Lee, M. T., Malaby, A. W., and Lambright, D. G. (2010) Specificity and membrane partitioning of Grsp1 signaling complexes with Grp1 family Arf exchange factors. *Biochemistry* **49,** 6083–6092
67. Gureasko, J., Kuchment, O., Makino, D. L., Sondermann, H., Bar-Sagi, D., and Kuriyan, J. (2010) Role of the histone domain in the autoinhibition and activation of the Ras activator Son of Sevenless. *Proc. Natl. Acad. Sci.*

U.S.A. **107,** 3430–3435
68. Jaiswal, M., Gremer, L., Dvorsky, R., Haeusler, L. C., Cirstea, I. C., Uhlenbrock, K., and Ahmadian, M. R. (2011) Mechanistic insights into specificity, activity, and regulatory elements of the regulator of G-protein signaling (RGS)-containing Rho-specific guanine nucleotide exchange factors (GEFs) p115, PDZ-RhoGEF (PRG), and leukemia-associated RhoGEF (LARG). *J. Biol. Chem.* **286,** 18202–18212
69. Mitin, N., Betts, L., Yohe, M. E., Der, C. J., Sondek, J., and Rossman, K. L. (2007) Release of autoinhibition of ASEF by APC leads to CDC42 activation and tumor suppression. *Nat. Struct. Mol. Biol.* **14,** 814–823
70. Scholz, R. P., Gustafsson, J. O., Hoffmann, P., Jaiswal, M., Ahmadian, M. R., Eisler, S. A., Erlmann, P., Schmid, S., Hausser, A., and Olayioye, M. A. (2011) The tumor suppressor protein DLC1 is regulated by PKD-mediated GAP domain phosphorylation. *Exp. Cell Res.* **317,** 496–503
71. Ching, Y. P., Wong, C. M., Chan, S. F., Leung, T. H., Ng, D. C., Jin, D. Y., and Ng, I. O. (2003) Deleted in liver cancer (DLC) 2 encodes a RhoGAP protein with growth suppressor function and is underexpressed in hepatocellular carcinoma. *J. Biol. Chem.* **278,** 10824–10830
72. Wong, C. M., Lee, J. M., Ching, Y. P., Jin, D. Y., and Ng, I. O. (2003) Genetic and epigenetic alterations of DLC-1 gene in hepatocellular carcinoma. *Cancer Res.* **63,** 7646–7651
73. Healy, K. D., Hodgson, L., Kim, T. Y., Shutes, A., Maddileti, S., Juliano, R. L., Hahn, K. M., Harden, T. K., Bang, Y. J., and Der, C. J. (2008) DLC-1 suppresses non-small cell lung cancer growth and invasion by RhoGAP-dependent and independent mechanisms. *Mol. Carcinog.* **47,** 326–337
74. Chan, F. K., Chung, S. S., Ng, I. O., and Chung, S. K. (2012) The RhoA GTPase-activating protein DLC2 modulates RhoA activity and hyperalgesia to noxious thermal and inflammatory stimuli. *Neurosignals* **20,** 112–126
75. Leung, T. H., Ching, Y. P., Yam, J. W., Wong, C. M., Yau, T. O., Jin, D. Y., and Ng, I. O. (2005) Deleted in liver cancer 2 (DLC2) suppresses cell transformation by means of inhibition of RhoA activity. *Proc. Natl. Acad. Sci. U.S.A.* **102,** 15207–15212
76. Kawai, K., Kiyota, M., Seike, J., Deki, Y., and Yagisawa, H. (2007) START-GAP3/DLC3 is a GAP for RhoA and Cdc42 and is localized in focal adhesions regulating cell morphology. *Biochem. Biophys. Res. Commun.* **364,** 783–789
77. Roof, R. W., Haskell, M. D., Dukes, B. D., Sherman, N., Kinter, M., and Parsons, S. J. (1998) Phosphotyrosine (p-Tyr)-dependent and -independent mechanisms of p190 RhoGAP-p120 RasGAP interaction: Tyr 1105 of p190, a substrate for c-Src, is the sole p-Tyr mediator of complex formation. *Mol. Cell. Biol.* **18,** 7052–7063
78. Gigoux, V., L'Hoste, S., Raynaud, F., Camonis, J., and Garbay, C. (2002) Identification of Aurora kinases as RasGAP Src homology 3 domain-binding proteins. *J. Biol. Chem.* **277,** 23742–23746
79. Yang, Y. S., Garbay, C., Duchesne, M., Cornille, F., Jullian, N., Fromage, N., Tocque, B., and Roques, B. P. (1994) Solution structure of GAP SH3 domain by ^{1}H NMR and spatial arrangement of essential Ras signaling-involved sequence. *EMBO J.* **13,** 1270–1279
80. Harkiolaki, M., Lewitzky, M., Gilbert, R. J., Jones, E. Y., Bourette, R. P., Mouchiroud, G., Sondermann, H., Moarefi, I., and Feller, S. M. (2003) Structural basis for SH3 domain-mediated high-affinity binding between Mona/Gads and SLP-76. *EMBO J.* **22,** 2571–2582